Application of the allylboration reaction of terminal acetylenes with allyldihaloboranes for the preparation of capping agents for the synthesis of precursors of polymeric iron(II) clathrochelates*

Ya. Z. Voloshin,[a] E. G. Lebed,[a] S. Yu. Erdyakov,[b] I. G. Makarenko,[a] K. A. Lyssenko,[a] Z. A. Starikova,[a] M. E. Gurskii,[b] and Yu. N. Bubnov[a,b]*

[a]*A. N. Nesmeyanov Institute of Organoelement Compounds, Russian Academy of Sciences, 28 ul. Vavilova, 119991 Moscow, Russian Federation. Fax: +7 (495) 135 5085. E-mail: voloshin@ineos.ac.ru*

[b]*N. D. Zelinsky Institute of Organic Chemistry, Russian Academy of Sciences, 47 Leninsky prosp., 119991 Moscow, Russian Federation. Fax: +7 (495) 135 5328. E-mail: bor@mail.ioc.ac.ru*

Template condensation on the iron(II) ion matrix of three cyclohexanedione-1,2-dioxime molecules with esters of 1,4-pentadienylboronic acids afforded apically functionalized bis(diolefin)-containing clathrochelates, which are new potential monomers for the preparation of functionalized carbochain polymers. The complexes were characterized by the data of elemental analysis, UV-Vis spectroscopy, ^{1}H, ^{11}B, and ^{13}C NMR spectroscopy, ^{57}Fe Mössbauer spectroscopy, IR spectroscopy, and MALDI-TOF mass spectrometry. The molecular and crystal structures of the clathrochelates synthesized and the electron density distribution on a molecule of one of them were determined by X-ray diffraction analysis.

Key words: macrocyclic compounds, clathrochelates, iron(II) complexes, organoboron compounds, monomers, X-ray diffraction analysis.

Clathrochelates, being macrobicyclic complexes with encapsulated metal cation, possess unusual chemical, physical, and physicochemical properties. This can be accounted for the metal ion encapsulation in the three-dimensional cavity of the macropolycyclic ligand that isolates it, to a great extent, from environmental factors.[1] The synthesis of clathrochelates containing olefinic substituents in capping fragments and capable of further participating in addition and polymerization processes is of undoubted interest for practical use of complexes of this type.

It has previously[1—8] been shown that boron compounds are the most appropriate capping agents for the direct template synthesis of tris-α-dioximate clathrochelates on the Fe^{2+} ion matrix. In the present work, we showed that the products of allylboration of terminal alkynes with allyldichloroboranes, *viz.*, 1,4-pentadienylboranes, can successfully be used as the capping agents in the syntheses of iron(II) clathrochelates that are derivatives of alicyclic cyclohexanedione-1,2-dioxime (nioxime). This dioxime was chosen because of easy formation and higher thermodynamic stability of the six- and eight-membered iron(II) alicyclic α-dioximates compared to their acyclic analogs.[9]

Results and Discussion

1,4-Pentadienylboranes are the products of the first step of classical allylboron-acetylene condensation, *viz.*, thermal reaction of acetylenes with triallyl- and tri(2-methylallyl)boranes,[10] can be isolated as individual compounds only in the case of alkoxyacetylenes (R = OMe, OEt) when temperature intervals of each of the three steps of this condensation differ substantially.[11] A simplest method to solve this problem is to carry out condensation in the so-called step-by-step version[12,13] using highly electrophilic allyldihaloboranes in the first step.[14] Diisopropyl esters of 1,4-pentadienylboronic acids (Scheme 1) are readily formed due to the alcoholysis of the products of allylboration of phenyl- and methylacetylenes, *viz.*, allyl- (**1**), methallyl- (**2**), and crotyldichloroboranes (**3**), with isopropyl alcohol, and their Lewis acidity can be used for the synthesis of macrobicyclic trisdioximates.

In most cases, boron-containing aliphatic and aromatic clathrochelate iron(II) trisdioximates have been synthesized[1] by the direct template condensation of the

* Dedicated to Academician O. M. Nefedov on the occasion of his 75th birthday.

Published in Russian in *Izvestiya Akademii Nauk. Seriya Khimicheskaya,* No. 11, pp. 1899—1909, November, 2006.

1066-5285/06/5511-1971

Scheme 1

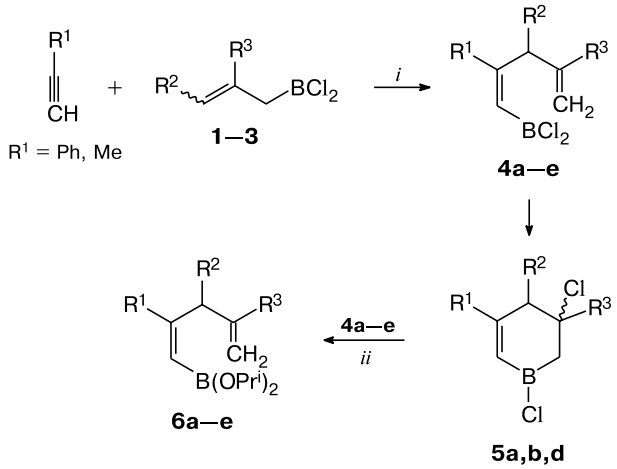

Reagents and conditions: *i*. CH_2Cl_2, −78 °C, 15 min; *ii*. Pr^iOH, Et_3N.

1: $R^2 = R^3 = H$; **2:** $R^2 = H$, $R^3 = Me$; **3:** $R^2 = Me$, $R^3 = H$

4—6	R^1	R^2	R^3	4—6	R^1	R^2	R^3
a	Ph	H	H	**d**	Me	H	Me
b	Ph	H	Me	**e**	Me	Me	H
c	Me	H	H				

corresponding α-dioxime and a boron-containing capping agent on the Fe^{2+} ion matrix. The reaction is usually carried out in polar protic solvents (first of all, alcohols) without addition of bases for binding of the releasing H^+ ions that formed. However, our attempts to synthesize bis(1,4-pentadienyl)clathrochelates under these conditions were unsuccessful because of the competing B—C bond protolysis in the initial boronates: this bond in alkylboranes readily undergoes protolytic cleavage.[10] Therefore, polar aprotic acetonitrile was chosen as the solvent for the macrocyclization reaction, and preliminarily synthesized non-macrocyclic trisnioximate $[Fe(H_2Nx)_3]Cl_2$ was used as the initial complex. However, side protolytic B—C bond cleavage was also observed in this system. Therefore, an equimolar amount of triethylamine was preliminarily added to solutions of 1,4-pentadienylboronates **6a—e** to neutralize acid that formed in the course of reaction.

Template capping of iron(II) nioximate $[Fe(H_2Nx)_3]Cl_2$ by boronates **6a—e** (Scheme 2) in acetonitrile in the presence of triethylamine made it possible to prepare complexes **7a—e** with the apical 1,4-pentadienyl substituents as a result of macrocyclization. Polymerization involving these complexes can be used for the synthesis of the corresponding polymeric systems.

Clathrochelates **7a—e** are intensely yellow-orange-colored finely crystalline compounds. Their structure and composition were confirmed by the data of elemental analysis, MALDI-TOF mass spectrometry, IR spectroscopy, and ^1H, ^{11}B, and ^{13}C NMR spectroscopy.

The ^1H and ^{13}C NMR spectra of solutions of the clathrochelates synthesized exhibit lines of the cyclohexane substituents in the α-dioximate fragments and characteristic signals of the apical R_B groups. The number and positions of the lines in these spectra, as well as the ratio of integral intensities of the signals in the ^1H NMR spectra, confirm the composition of the complexes and symmetry of their molecules. The broadened signals of the capping boron atoms in the ^{11}B NMR spectra have chemical shifts at ~6 ppm (relative to $BF_3 \cdot OEt_2$), which are characteristic of the tetrahedral boron atom in the O_3BC moiety.

The IR spectra of the complexes synthesized exhibit both the characteristic of the boron-containing trisdioximate clathrochelates bands of stretching vibrations of the C=N, N—O, and B—O bonds and the bands of stretching vibrations of the C=C bonds in the apical substituents.

Scheme 2

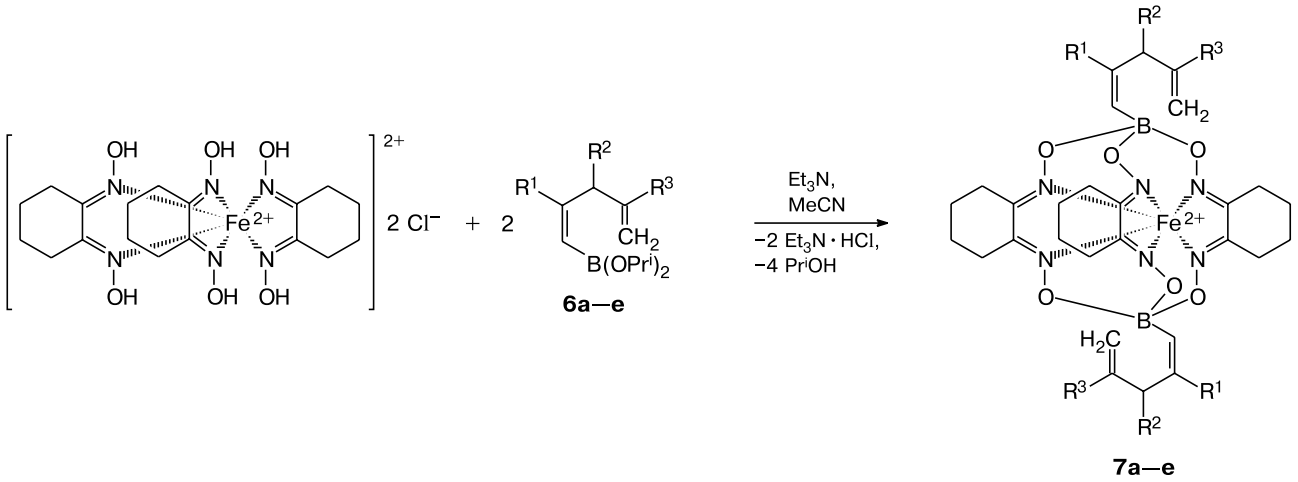

Table 1. Selected structural data and ^{57}Fe Mössbauer parameters for the trisdioximate clathrochelates synthesized and their analogs

Complex	IS[a]	QS[b]	Fe—N/Å	φ/deg	*h*/Å	α/deg
	mm s^{-1}					
7a	0.31	0.73	1.91	21.2	2.35	39.3
7b	0.32	0.68				
7c	0.32	0.54	1.91	20.6	2.36	39.3
7d	0.30	0.56	1.90	20.6	2.36	39.3
7e	0.31	0.54				
$FeNx_3(BcpFecp)_2 \cdot 2CCl_4$[15]	0.31	0.72 (Fe^{2+})	1.90	9.5	2.38	39.3
	0.70	2.36 (cpFecp)				
$FeNx_3(BBu^n)_2$[16]	0.32	0.58	1.91	20.3	2.34	39.1
$FeNx_3(BCH_2CH{=}CH_2)_2$ (type A)[17]	0.28	0.74	1.90	13.8	2.36	38.9
(type B)				17.0		
$FeNx_3(B\textit{n}\text{-}C_{16}H_{33})_2$ at 298 K, (type A)[17]	0.31	0.68	1.91	10	2.37	38.9
(type B)			1.91	18	2.35	
$FeNx_3(BC_6H_3(OMe)_2)_2 \cdot CHCl_3$[18]	0.31	0.84	1.90	17.8	2.35	39.1
$FeNx_3(BC{\equiv}CPh)_2 \cdot PhCH_3$ (type A)[18]	0.33	0.67	1.90	11.4	2.36	38.7
(type B)			1.91	19.8	2.35	39.1

[a] Isomeric shift.
[b] Quadrupole splitting.

The UV-Vis spectra of solutions of the compounds synthesized contain charge-transfer Fed → Lπ* bands in the clathrochelate framework (less intense (ε ≈ 2—3 · 10^3 L mol^{-1} cm^{-1}) in the region of 420—430 nm and more intense (ε ≈ 1—2 · 10^4 L mol^{-1} cm^{-1}) at ~450 nm) and, hence, they virtually coincide. The bands in the UV region belong to π—π*-transitions in both the π-conjugated α-dioximate chelate cycles and 1,4-pentadienyl apical substituents. Therefore, in the case of the phenyl-containing apical substituents at the capping boron atom, the intensity of the short-wavelength bands in the spectra of the synthesized clathrochelates increases substantially due to conjugation of the π-systems of the Ph groups and 1,4-pentadienyl fragments.

The parameters of the ^{57}Fe Mössbauer spectra of the clathrochelates synthesized (Table 1) characterize them as the low-spin iron(II) complexes, geometry of which is intermediate between the trigonal prism (TP) (distortion angle φ = 0°) and trigonal antiprism (TAP) (φ = 60°). This conclusion was confirmed by the X-ray diffraction data for three of the five complexes synthesized.

The molecular structures of clathrochelates **7a**, **7c**, and **7d** with the apical 1,4-pentadienyl substituents are shown in Figs 1—3. Although molecule **7c** lies on the 2-fold axis and molecule **7d** is in general position, the distortion of the TP of the coordination polyhedron of the iron(II) ion is the same: the distortion angles φ in this polyhedron are 20.6°, and the *h* heights of the TPs of the coordination polyhedra are 2.36 and 2.35 Å, respectively. In molecule **7a** the φ and *h* values are 21.2° and 2.35 Å, respectively.

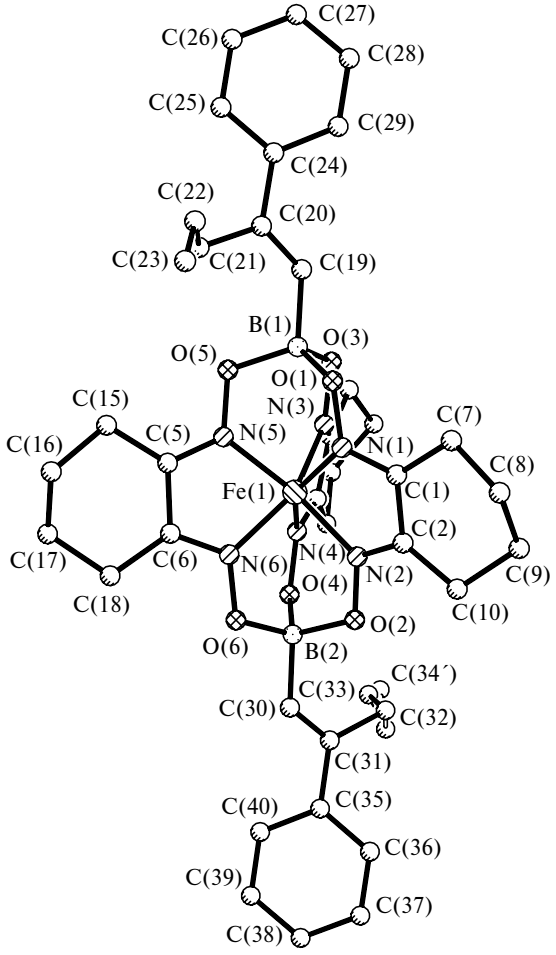

Fig. 1. Molecular structure of clathrochelate **7a**.

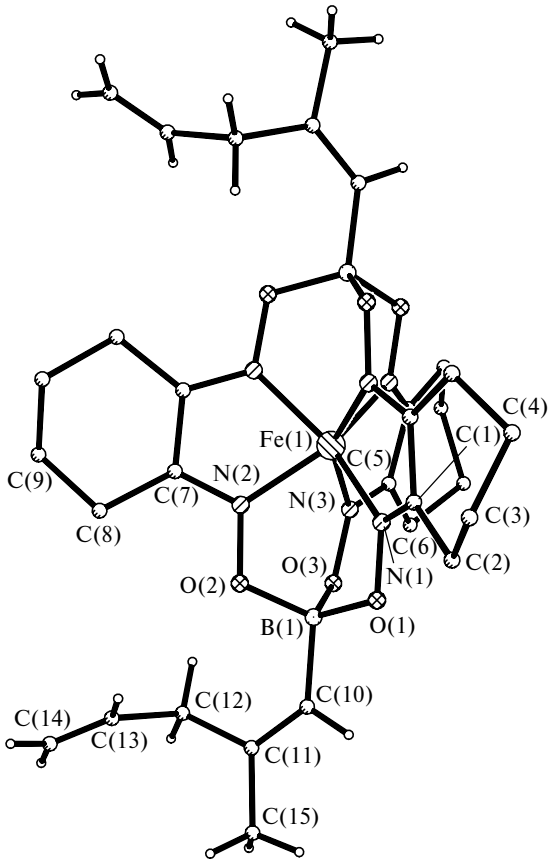

Fig. 2. Molecular structure of clathrochelate **7c**.

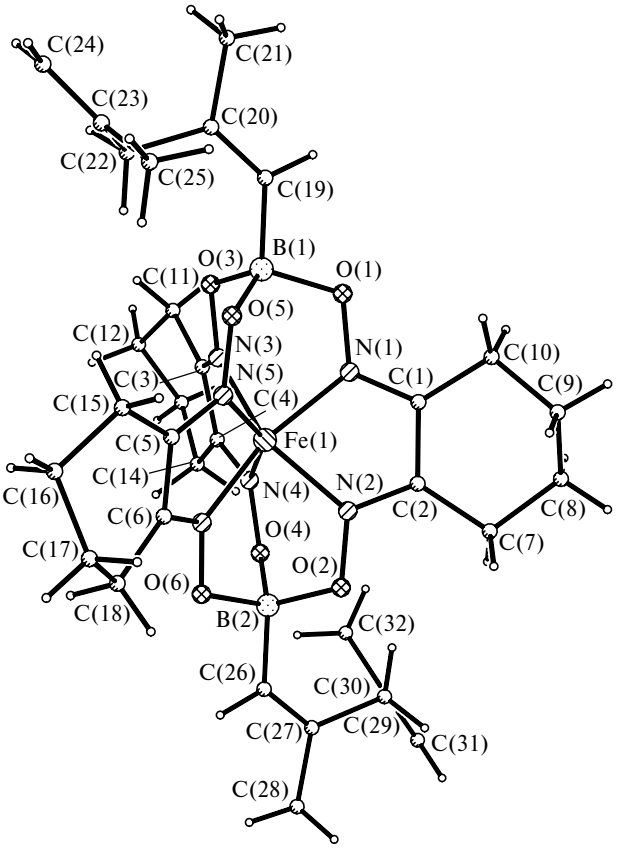

Fig. 3. Molecular structure of clathrochelate **7d**.

The geometric characteristics of the apical substituents are close in all the molecules studied by X-ray diffraction, but their mutual orientations differ (Table 2). In molecules **7a** and **7d** the 1,4-pentadienyl substituents are coplanar but oriented in opposite directions, while in molecule **7c** they are turned relative to each other by 61°. Intramolecular contacts of the methylene units of the $BC{=}CRCH_2$ fragments with the oxygen atoms of the tripode capping O_3BC groups are determining for the orientation of the apical substituents relative to the clathrochelate framework. The R^1 substituent is always perpendicular to the plane of the 1,4-pentadienyl fragment.

Table 2. Selected geometric parameters of the apical 1,4-pentadienyl substituents $C(1){=}C(2)(—C(6)(R^2))—C(3)—C(4)(R^3){=}C(5)$ in crystals of **7a,c,d**

Parameter	**7a**	**7c**	**7d**
Bond		*d*/Å	
B—C(1)	1.584(3), 1.586(3)	1.584(2)	1.579(5), 1.570(5)
C(1)=C(2)	1.338(3), 1.332(3)	1.335(2)	1.336(5), 1.319(5)
C(2)—C(6)	1.490(3), 1.489(3) (R^2 = Ph)	1.508(3) (R^2 = Me)	1.508(5), 1.518(5) (R^2 = Me)
C(2)—C(3)	1.516(3), 1.520(3)	1.513(3)	1.503(5), 1.517(5)
C(3)—C(4)	1.500(3), 1.490(4)* (R^3 = H)	1.504(1)* (R^3 = H)	1.504(5), 1.508(5) (R^3 = Me)
C(4)=C(5)	1.307(4), 1.307(7)*	1.313(5)*	1.330(5), 1.307(6)
B(1)—O	1.492(3), 1.498(3), 1.508(3)	1.509(2), 1.497(2), 1.504(2)	1.504(4), 1.496(4), 1.505(4)
B(2)—O	1.512(3), 1.500(3), 1.498(3)		1.499(4), 1.509(4), 1.507(5)
Angle		ω/deg	
O—B(1)—O	109.3(2), 110.6(2), 108.8(2)	109.4(1), 109.5(1), 109.4(1)	109.7(3), 109.1(3), 109.5(3)
O—B(2)—O	108.9(2), 109.3(2), 110.3(2)		108.4(3), 109.2(3), 108.9(3)
O—B(1)—C(6)	110.2(2), 106.2(2), 111.6(2)	107.0(1), 110.5(1), 111.0(1)	105.9(3), 110.8(3), 111.7(3)
O—B(2)—C(6)	110.2(2), 110.0(2), 108.1(2)		112.8(3), 110.9(3), 106.6(3)

* Disordered atoms.

Thus, variation of the apical substituents in the clathrochelate molecules under study exerts no substantial effect on the geometry of the clathrochelate framework but results in differences in their crystal packing due to a change in the general shape of the molecules.

The effect of the nature of solvate molecules on the supramolecular organization of crystals of the clathrochelates of this type was studied for complex **7a**. The structure of clathrochelate molecule **7a** (see Fig. 1) is the same in all the three crystals formed by this clathrochelate and determined by X-ray diffraction analysis, except for disordering of one of the allyl fragments of the 1,4-pentadienyl substituents in crystals **7a** and **7a** · C_6H_6. In addition to the disordering of the allyl fragment, the clathrochelate molecules in these structures differ by mutual orientation of these apical substituents $CH{=}CPhCH_2CH{=}CH_2$: in crystals **7a** and **7a** · $CHCl_3$ the Ph groups are virtually coplanar (dihedral angles between their planes are 8.7 and 12.8°, respectively), whereas in molecule **7a** · C_6H_6 this angle is 79.9° (Table 3).

Selected geometric parameters of the clathrochelate framework of **7a** presented in Tables 1 and 3 are the same in all the three crystals. The distortion angles (φ) of the TP of the coordination polyhedron in crystals **7a**, **7a** · $CHCl_3$, and **7a** · C_6H_6 are given in Table 3. The presence of solvate molecules exerts no substantial effect on the φ angle value: in non-solvated crystal **7a** the distortion angle is by ~1° larger than that in solvate-containing crystals **7a** · $CHCl_3$ and **7a** · C_6H_6.

The clathrochelate molecule is whirligig: the diameter of the central belt (toroid) is ~9.5 Å and the axis length is 19.5 Å. In all the three crystals, the clathrochelate molecules are arranged in such a way that the C_3 axes of the molecules are parallel. Crystal packing in non-solvated crystal **7a** is determined by standard van der Waals interactions between the atoms of the peripheral groups. Since molecules of this shape are poorly packed in crystal, the crystal contains free cavities (Fig. 4). The largest centrosymmetric cavity is observed in the cell center: its approximate size is 5.2×7.8×8.5 $Å^3$.

In crystal **7a** · $CHCl_3$ the solvate chloroform molecules are disordered over two positions (site occupancy is close to 0.7 : 0.3) and form the O(5)...$HCCl_3$ hydrogen bond with the clathrochelate molecules (O...H distances are 2.36 and 2.29 Å for two disordered molecules). The solvate chloroform molecules are included into the centrosymmetric cavity (Fig. 5) thus increasing its size. The formation of layers of the clathrochelate molecules parallel to the *ac* plane and surrounded by the solvate chloroform molecules bonded with them through the hydrogen bond are clearly seen (Fig. 6).

In crystals **7a** · C_6H_6 similar layers of clathrochelate molecules are more distant and the solvate benzene molecules are arranged between these layers parallel to the *ab* plane (Fig. 7). Crystal **7a** · C_6H_6 is least densely packed: d_{calc} = 1.396 (**7a**), 1.407 (**7a** · $CHCl_3$), and 1.332 g cm^{-3} (**7a** · C_6H_6). Thus, the inclusion of solvate molecules into the crystal structure of the clathrochelate molecules decreases the density of its packing to form the layers of the clathrochelate molecules.

In crystals formed by clathrochelate **7a**, the deviation of the iron(II) ion from the center of the coordination N_6 polyhedron does not exceed 0.001 Å. Therefore, these

Table 3. Selected geometric parameters of the clathrochelate molecules in crystals of **7a**, **7a** · $CHCl_3$, and **7a** · C_6H_6

Parameter	**7a**	**7a** · $CHCl_3$	**7a** · C_6H_6
Bond		*d*/Å	
Fe—N(1)	1.913(2)	1.912(1)	1.906(1)
Fe—N(2)	1.906(2)	1.909(1)	1.911(1)
Fe—N(3)	1.911(2)	1.912(1)	1.904(2)
Fe—N(4)	1.900(2)	1.915(1)	1.908(2)
Fe—N(5)	1.899(2)	1.912(1)	1.916(2)
Fe—N(6)	1.910(2)	1.910(1)	1.911(1)
N(1)—O(1)	1.378(2)	1.371(1)	1.374(2)
N(2)—O(2)	1.374(2)	1.376(1)	1.372(2)
N(3)—O(3)	1.371(2)	1.377(1)	1.371(2)
N(4)—O(4)	1.376(2)	1.372(1)	1.372(2)
N(5)—O(5)	1.375(2)	1.378(1)	1.372(2)
N(6)—O(6)	1.368(2)	1.370(1)	1.380(2)
B(1)—O(1)	1.492(3)	1.494(2)	1.500(2)
B(1)—O(3)	1.498(3)	1.500(2)	1.510(2)
B(1)—O(5)	1.508(3)	1.511(2)	1.500(2)
B(2)—O(2)	1.512(3)	1.505(2)	1.504(2)
B(2)—O(4)	1.500(3)	1.503(2)	1.501(2)
B(2)—O(6)	1.498(3)	1.498(2)	1.501(2)
N(1)—C(1)	1.304(3)	1.305(2)	1.302(2)
N(2)—C(2)	1.308(3)	1.306(2)	1.309(2)
N(3)—C(3)	1.310(3)	1.309(2)	1.309(2)
N(4)—C(4)	1.311(3)	1.308(2)	1.305(2)
N(5)—C(5)	1.307(3)	1.310(2)	1.307(2)
N(6)—C(6)	1.306(3)	1.308(2)	1.305(2)
C(1)—C(2)	1.445(3)	1.442(2)	1.438(2)
C(3)—C(4)	1.433(3)	1.437(2)	1.434(3)
C(5)—C(6)	1.436(3)	1.439(2)	1.440(2)
h/Å	2.35	2.36	2.36
Angle		ω/deg	
N(1)...Fe...N(2)	178.1	178.7	178.7
Ph(1)...Ph(2)*	8.7	12.8	79.9
C(19)—C(20)—C(21)—C(22)	124.7(2)	105.1(1)	127.2(3), 98.6(8)**
C(20)—C(21)—C(22)—C(23)	54.3(3)	120.4(2)	70.7(3), 112.7(1)**
C(30)—C(31)—C(32)—C(33)	81.7(3), 50(1)**	105.9(1)	92.3(2)
C(31)—C(32)—C(33)—C(34)	75.5(3), 118(2)**	114.7(2)	137.8(2)
Distortion angle		φ/deg	
	21.2	19.8	20.2

* Angle between the planes of the phenyl substituents.
** The allyl fragment is disordered.

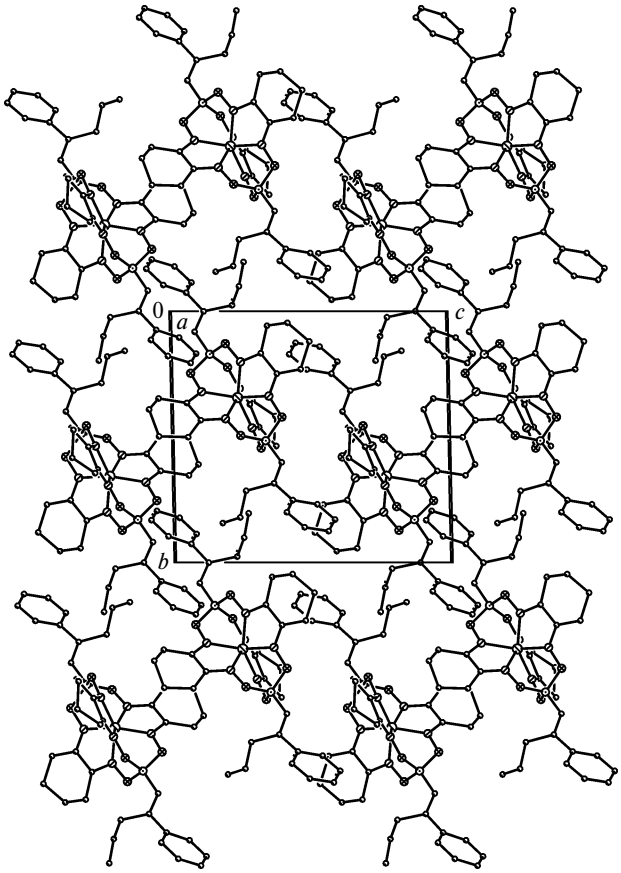

Fig. 4. Crystal packing of **7a** (projection on the *bc* plane).

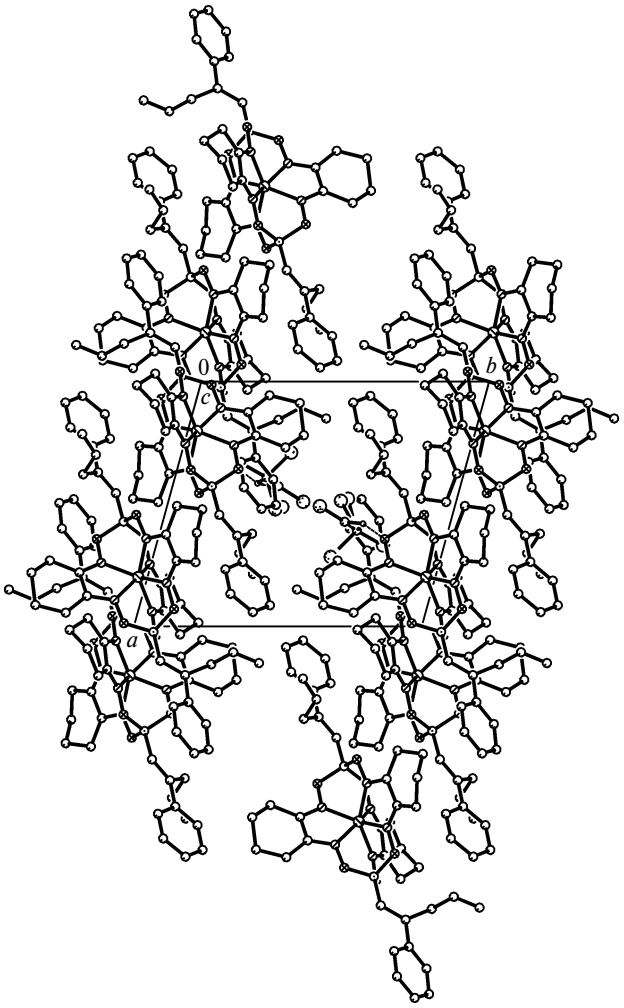

Fig. 5. Crystal packing of **7a** · $CHCl_3$ (projection on the *ab* plane).

crystals are attractive for high-resolution X-ray diffraction studies: the absence of considerable distortions in the clathrochelate framework will allow the effect of ribbed

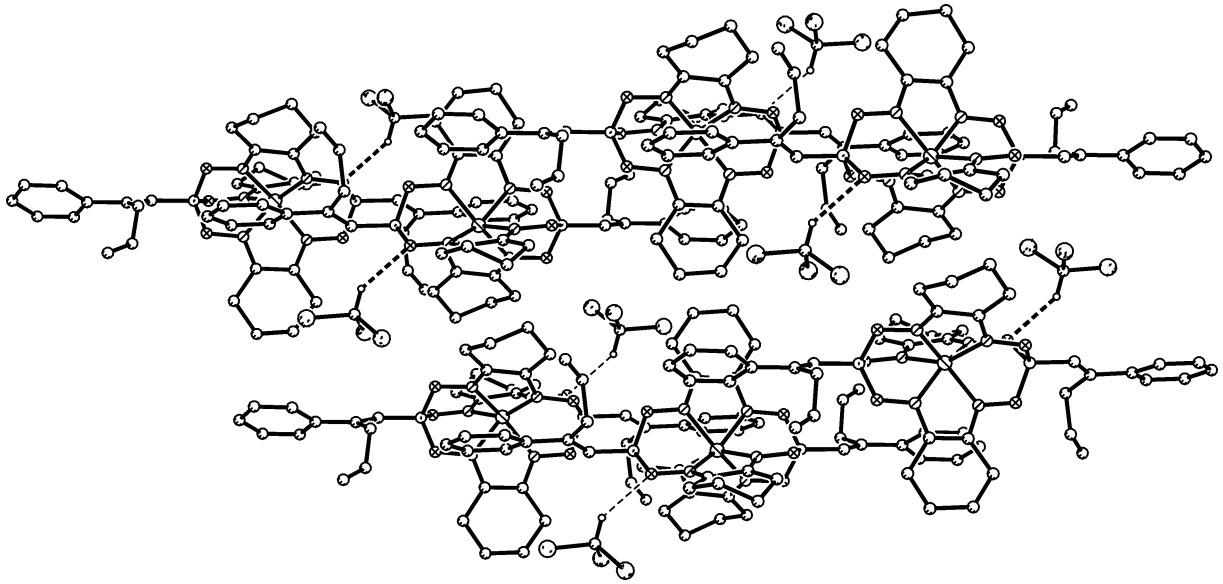

Fig. 6. Localization of solvate chloroform molecules near the layer of clathrochelate molecules **7a** and hydrogen bond formation in crystal **7a** · $CHCl_3$.

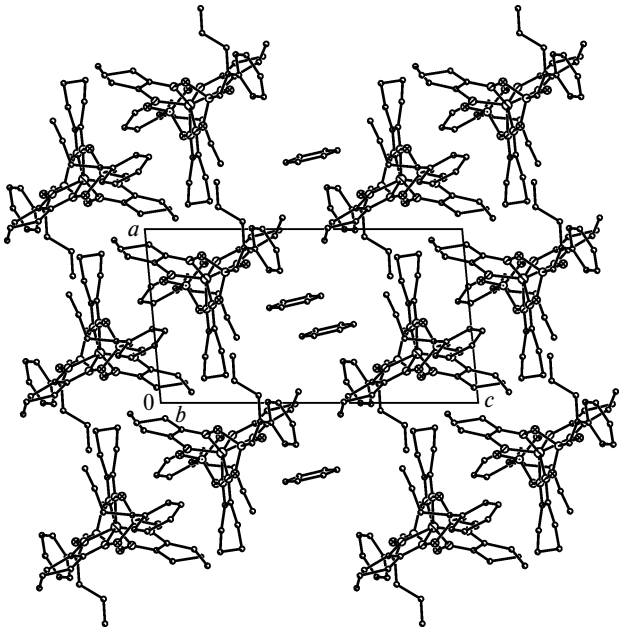

Fig. 7. Crystal packing of clathrochelate and solvate molecules **7a** · C_6H_6 (projection on the *ac* plane).

functionalization of the clathrochelate on the character of the Fe—N chemical bond and occupancy of the 3d-orbitals of the iron(II) ion to be determined more distinctly in future.

The crystals most appropriate for this study were obtained for the chloroform solvate **7a** · $CHCl_3$ in which the function of the electron density distribution ρ(**r**) was recovered with very high accuracy despite disordering of the solvate molecule.

Analysis of the deformation electron density (DED) distribution showed that distribution anisotropy, which is characteristic of transition metal ions, is observed in the vicinity of the iron atom. The DED maxima lie in the plane passing through the middles of the C(1)—C(2), C(3)—C(4), and C(5)—C(6) bonds (Fig. 8, *a*) and along the lines connecting the encapsulated iron ion and capping boron atoms (Fig. 8, *b*). As can be seen from the presented cross sections, the organoelement clathrochelate framework is characterized by the expected features of the DED distribution: the maxima are localized on the chemical bonds and near lone electron pairs of the nitrogen and oxygen atoms. Ellipticity of the maxima corresponding to the DED accumulation in the middle of the C—C bond (see Fig. 8, *a*) indicates a substantial contribution of the π-component to bonds of this type. Another interesting feature of these cross sections is a considerable polarization of electron pairs of the nitrogen atom and a continuous distribution connecting the electron pairs of the nitrogen atoms and the DED maximum corresponding to the d-orbitals of the iron atom. Similar character of the DED distribution and the presence of the π-component of the C—C bond in the chelate fragment indicate, in

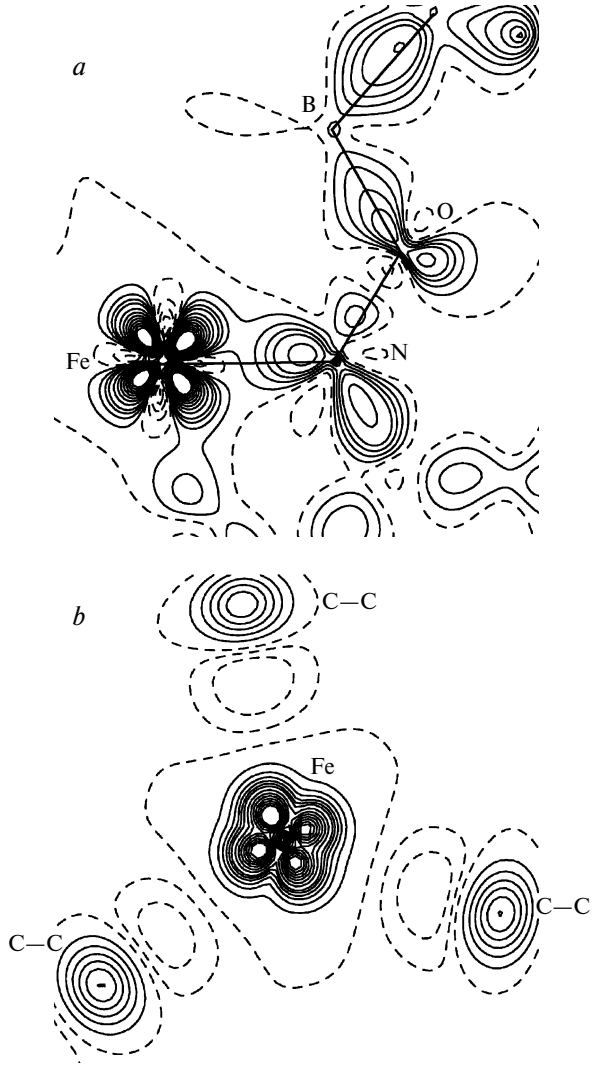

Fig. 8. Cross-sections of DED in the plane passing through the Fe, N(1), and B(1) atoms (*a*) and through the middles of the C(1)—C(2), C(3)—C(4), and C(5)—C(6) bonds (*b*). The contours are drawn with an increment of 0.1 e $Å^{-3}$, and the negative isolines are dashed.

turn, a substantial electron delocalization in the five-membered chelate metallocycles (Fig. 9).

To obtain more detailed information on the character of interactions in molecule **7a**, we performed topological analysis of ρ(**r**) in terms of the Bader theory ("Atoms in Molecules"). Search for critical points (CPs) (3, −1) showed that the presence of CPs (3, −1) in the region of all expected interactions including the Fe—N bond. In addition to CPs (3, −1), numerous CPs (3, +1) were also localized in molecule **7a**. They correspond to closure of three saturated and three aromatic six-membered cycles, three five-membered chelate metallocycles, and six six-membered FeN_2O_2B type cycles. Two polyhedral CPs (3, +3) are localized along the Fe...B straight lines. All CPs (3, +1) and CPs (3, +3) were localized at a con-

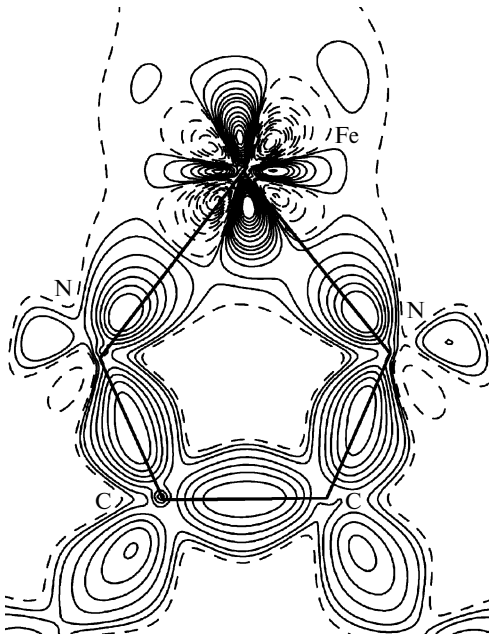

Fig. 9. DED distribution in the five-membered chelate metallocycle. The contours are drawn with an increment of 0.1 e Å^{-3}, and the negative isolines are dashed.

siderable distance from CPs (3, −1), indicating that this molecular graph is stable.

Charges of the atoms in molecule **7a** were determined by integration of atomic basins. The values of the Lagrangian ($-1/4\nabla^2\rho(\mathbf{r})$) integrated by atomic basins can confirm the accuracy of the atomic basins. In particular, in the case of the iron ion, the Lagrangian equals $1 \cdot 10^{-4}$ au and differs minimally from the expected zero value. The obtained charge values show that the main negative charge in the clathrochelate cage is localized on the oxygen (−0.92 *e*) and nitrogen (−0.61 *e*) atoms, and the positive charge is localized on the boron atoms (+2.23 *e*) and carbon atoms of the five-membered chelate metallocycle (+0.40 *e*). Although the formal oxidation state is +2, the charge of the iron atom is +0.63 *e*, which is close to that of the iron atom in ferrocene (0.79 *e*) according to the quantum chemical calculation.[19]

Analysis of the topological parameters in CPs (3, −1) showed that the Fe—N bonds, as in the earlier studied coordination compounds,[20] correspond to an intermediate type of interactions. Indeed, despite positive values of the Laplacian of the electron density ($\nabla^2\rho(\mathbf{r}) \approx 11.84$ e Å^{-5}) in CPs (3, −1), the $\rho(\mathbf{r})$ values are rather high (0.79 e Å^{-3}) and the local energy density is negative ($h_e(\mathbf{r}) \approx -0.037$ au).

The ellipticity values (ε) for the Fe—N bonds (0.09) are lower than the corresponding values for the C—C (0.18) and N—C (0.26) bonds in the chelate metallocycles; however, they, as well as the DED maps mentioned above, indicate the electron delocalization in the chelate cycles.

Thus, based on the above-mentioned analysis of $\rho(\mathbf{r})$ in crystal **7a**, we obtained the data on the character of interactions of the encapsulated iron(II) ion with the donor nitrogen atoms of the clathrochelate framework and observed the charge delocalization in the chelate metallocycles.

This study showed that 1,4-pentadienylboronic acids and their derivatives can successfully be used as capping agents in syntheses of the iron(II) clathrochelates that are precursors of functionalized linear and cross-linked carbochain polymers.

Experimental

The following commercial reagents were used: $FeCl_2 \cdot 4H_2O$, triethylamine, and cyclohexanedione-1,2-dioxime (nioxime, H_2Nx) (Fluka). The $[Fe(H_2Nx)_3]Cl_2$ complex was synthesized by an earlier described procedure,[21] and diisopropyl esters of 1,4-pentadienylboronic acids were synthesized as described previously.[12,22]

The contents of C, H, and N were determined on a Carlo Erba microanalyzer (model 1106); iron was determined spectrophotometrically.

MALDI-TOF mass spectra were recorded with a MALDI-TOF-MS Autoflex Bruker time-of-flight mass spectrometer in the reflecto-mol operation mode. Ionization of particles was induced by an UV laser with the wavelength 336 nm. A nickel plate served as the target, and 2,5-dihydroxybenzoic acid was used as a matrix. The measurement accuracy was 0.1%.

IR spectra (KBr pellets) in the range of 400—4000 cm^{-1} were recorded with an IR200 Thermo Nicolet FT spectrophotometer.

UV-Vis spectra of solutions of the complexes in CH_2Cl_2 in a range of 230—900 nm were obtained with a Perkin—Elmer Lambda 9 spectrophotometer. The spectra were decomposed into the Gauss components using the SPECTRA program.

^{1}H, ^{11}B, and ^{13}C NMR spectra were recorded on a Bruker AC-200 P spectrometer (working frequencies 200.13, 64.21, and 50.32 MHz on the ^{1}H, ^{11}B, and ^{13}C nuclei, respectively) in $CDCl_3$ and CD_2Cl_2.

^{57}Fe Mössbauer spectra were obtained with an YaGRS-4M spectrometer with constant acceleration mode. The spectra were collected with a 256-channel analyzer. Isomeric shifts were measured relative to sodium nitroprusside, and an α-Fe foil was used for velocity scale calibration. The radiation source was ^{57}Co in a chromium matrix, which was always kept at room temperature. The minimum absorption linewidth in the spectrum of a standard sodium nitroprusside sample was 0.24 mm s^{-1}.

1,12-Bis(2-phenylpenta-1,4-dienylbora)-2,11,13,22,23,32-hexaoxa-3,10,14,21,24,31-hexaazapentacyclo-[11.11.11.0$^{4.9}$0^{15,20}0$^{25.30}$]ditriaconta-3,9,14,20,24,30-hexane(2−)iron(II) (7a). Complex $[Fe(H_2Nx)_3]Cl_2$ (0.45 g, 1 mmol) was dissolved/suspended in acetonitrile (1 mL), and a solution of Et_3N (0.21 g, 2.09 mmol) and boronate **6a** (0.57 g, 2.09 mmol) in acetonitrile (2 mL) was added dropwise with stirring under argon. The reaction mixture was stirred for 4 h and left for 16 h at 4 °C. A precipitate that formed was filtered, washed with a small amount of acetonitrile, and dissolved in methylene chloride. The solution was filtered through a layer of silica gel SPH-300 and evaporated to dryness. The solid residue was washed with hexane and dried *in vacuo*. The yield was 0.54 g

(71%). Found (%): C, 61.11; H, 5.96; N, 10.69; Fe, 6.96. $C_{40}H_{46}N_6O_6B_2Fe$. Calculated (%): C, 61.25; H, 5.92; N, 10.71; Fe, 7.12. Mass spectrum: *m/z* 784 $[M]^{\bullet+}$. ^1H NMR (CD_2Cl_2), δ: 1.69 (br.s, 12 H, β-CH_2 (Nx)); 2.78 (br.s, 12 H, α-CH_2 (Nx)); 3.43 (d, 4 H, CH_2 (R_B)*, $J_{H,H}$ = 6.2 Hz); 4.85 (m, 4 H, =CH_2 (R_B)); 5.80 (s, 2 H, BCH (R_B)); 5.83 (m, 2 H, =CH (R_B)); 7.15 (m, 6 H, Ph (R_B)); 7.37 (m, 4 H, Ph (R_B)). $^{13}C\{^1H\}$ NMR (CD_2Cl_2), δ: 21.9 (β-CH_2 (Nx)); 26.5 (α-CH_2 (Nx)); 37.8 (CH_2 (R_B)); 115.0 (=CH_2 (R_B)); 126.5, 126.8, 128.2 (Ph (R_B)); 139.3 (=CH (R_B)); 144.3 (Ph (R_B)); 149.0 (=CPh (R_B)); 151.7 (C=N). IR (KBr), ν/cm^{-1}: 910, 935, 1057 (N—O), 1111 m (B—O), 1572 (C=N), 1622 m (C=C). UV-Vis ($CHCl_3$), λ_{max}/nm (ε · 10^{-3}/L mol^{-1} cm^{-1}): 250 (35), 287 (23), 308 (4.9), 350 (2.6), 424 (3.5), 452 (16).

1,12-Bis(4-methyl-2-phenylpenta-1,4-dienylbora)-2,11,13,22,23,32-hexaoxa-3,10,14,21,24,31-hexaazapentacyclo[11.11.11.$0^{4.9}0^{15,20}0^{25.30}$]ditriaconta-3,9,14,20,24,30-hexaene(2−)iron(II) (7b). Complex $[Fe(H_2Nx)_3]Cl_2$ (0.56 g, 1 mmol) was dissolved/suspended in acetonitrile (2 mL), and a solution of Et_3N (0.21 g, 2 mmol) and boronate **6c** (0.59 g, 2 mmol) in acetonitrile (1 mL) was added dropwise with stirring under argon. The reaction mixture was stirred for 4 h and left for 16 h at 4 °C. The target clathrochelate was isolated in the same manner as complex **7a**. The yield was 0.28 g (35%). Found (%): C, 61.87; H, 6.23; N, 10.19; Fe, 6.82. $C_{34}H_{50}B_2FeN_6O_{10}$. Calculated (%): C, 62.09; H, 6.21; N, 10.35; Fe, 6.87. Mass spectrum: *m/z* 812 $[M]^{\bullet+}$. ^1H NMR ($CDCl_3$), δ: 1.72 (s, 6 H, Me (R_B)); 1.79 (br.s, 12 H, β-CH_2 (Nx)); 2.92 (br.s, 12 H, α-CH_2 (Nx)); 3.58 (s, 4 H, CH_2 (R_B)); 4.74 (m, 4 H, =CH_2 (R_B)); 6.00 (s, 2 H, BCH (R_B)); 7.22 (m, 6 H, Ph (R_B)); 7.50 (m, 4 H, Ph (R_B)). $^{13}C\{^1H\}$ NMR ($CDCl_3$), δ: 21.6 (β-CH_2 (Nx)); 22.6 (Me (R_B)); 26.2 (α-CH_2 (Nx)); 41.3 (CH_2 (R_B)); 111.4 (=CH_2 (R_B)); 126.3, 126.8, 127.6, 144.0 (Ph (R_B)); 144.8 (=CMe (R_B)); 149.0 (=CPh (R_B)); 151.2 (C=N). IR (KBr), ν/cm^{-1}: 931 m, 1057 (N—O), 1109 m (B—O), 1572 (C=N), 1614 m (C=C). UV-Vis ($CHCl_3$), λ_{max}/nm (ε · 10^{-3}/L mol^{-1} cm^{-1}): 249 (22), 287 (14), 308 (3.4), 359 (1.9), 425 (2.2), 453 (11).

1,12-Bis(2-methylpenta-1,4-dienylbora)-2,11,13,22,23,32-hexaoxa-3,10,14,21,24,31-hexaazapentacyclo-[11.11.11.$0^{4.9}0^{15,20}0^{25.30}$]ditriaconta-3,9,14,20,24,30-hexaene(2−)iron(II) (7c). Complex $[Fe(H_2Nx)_3]Cl_2$ (0.34 g, 0.61 mmol) was dissolved (suspended) in acetonitrile (1 mL), and a solution of Et_3N (0.25 g, 2.4 mmol) and boronate **6c** (0.52 g, 2.4 mmol) in acetonitrile (2 mL) was added dropwise with stirring under argon. The reaction mixture was stirred for 4 h and left for 16 h at 4 °C. The target product was isolated in the same manner as complex **7a**. The yield was 0.13 g (33%). Found (%): C, 54.59; H, 6.51; N, 12.61; Fe, 8.40. $C_{30}H_{42}N_6O_6B_2Fe$. Calculated (%): C, 54.57; H, 6.42; N, 12.73; Fe, 8.46. Mass spectrum: *m/z* 660 $[M]^{\bullet+}$. ^1H NMR ($CDCl_3$), δ: 1.78 (s, 6 H, Me (R_B)); 1.81 (br.s, 12 H, β-CH_2 (Nx)); 2.88 (br.s, 12 H, α-CH_2 (Nx)); 3.02 (d, 4 H, CH_2 (R_B), $J_{H,H}$ = 6.8 Hz); 5.02 (m, 4 H, =CH_2 (R_B)); 5.28 (s, 2 H, BCH (R_B)); 5.89 (m, 2 H, =CH (R_B)). $^{13}C\{^1H\}$ NMR ($CDCl_3$), δ: 21.6 (β-CH_2 (Nx)); 25.6 (Me (R_B)); 26.1 (α-CH_2 (Nx)); 41.0 (CH_2 (R_B)); 114.7 (=CH_2 (R_B)); 138.9 (=CH (R_B)); 147.9 (=CMe (R_B)); 151.0 (C=N). IR (KBr), ν/cm^{-1}: 908, 930, 1059 m (N—O), 1119 m (B—O), 1576 (C=N), 1631, 1649 (C=C). UV-Vis ($CHCl_3$), λ_{max}/nm (ε · 10^{-3}/L mol^{-1} cm^{-1}): 251 (12), 283 (10), 305 (3.3), 341 (2.3), 409 (2.0), 450 (17).

1,12-Bis(2,4-dimethylpenta-1,4-dienylbora)-2,11,13,22,23,32-hexaoxa-3,10,14,21,24,31-hexaazapentacyclo[11.11.11.$0^{4.9}0^{15,20}0^{25.30}$]ditriaconta-3,9,14,20,24,30-hexaene(2−)iron(II) (7d). Complex $[Fe(H_2Nx)_3]Cl_2$ (0.3 g, 0.54 mmol) was dissolved/suspended in acetonitrile (1 mL), and a solution of Et_3N (0.22 g, 2.2 mmol) and boronate **5d** (0.43 g, 2.2 mmol) in acetonitrile (2 mL) was added dropwise with stirring under argon. The reaction mixture was stirred for 3 h and left for 16 h at 4 °C. The target clathrochelate was isolated as described above for complex **7a**. The yield was 0.13 g (36%). Found (%): C, 55.75; H, 6.68; N, 12.29; Fe, 8.07. $C_{32}H_{46}N_6O_6B_2Fe$. Calculated (%): C, 55.84; H, 6.75; N, 12.21; Fe, 8.11. Mass spectrum: *m/z* 688 $[M]^{\bullet+}$. ^1H NMR ($CDCl_3$), δ: 1.75 (m, 18 H, β-CH_2 (Nx) + Me (R_B)); 1.79 (s, 6 H, Me (R_B)); 2.87 (br.s, 12 H, α-CH_2 (Nx)); 3.04 (s, 4 H, CH_2 (R_B)); 4.77 (m, 4 H, =CH_2 (R_B)); 5.33 (s, 2 H, BCH (R_B)). $^{13}C\{^1H\}$ NMR ($CDCl_3$), δ: 21.6 (β-CH_2 (Nx)); 22.0, 25.3 (Me (R_B)); 26.1 (α-CH_2 (Nx)); 44.7 (CH_2 (R_B)); 111.0 (=CH_2 (R_B)); 145.4, 147.4 (=CMe (R_B)); 151.0 (C=N). IR (KBr), ν/cm^{-1}: 930 m, 1041, 1061 (N—O), 1117 m (B—O), 1576 (C=N), 1637 m (C=C). UV-Vis ($CHCl_3$), λ_{max}/nm (ε · 10^{-3}/L mol^{-1} cm^{-1}): 251 (11), 284 (9.4), 305 (3.2), 360 (2.4), 423 (2.3), 452 (16).

1,12-Bis(2,3-dimethylpenta-1,4-dienylbora)-2,11,13,22,23,32-hexaoxa-3,10,14,21,24,31-hexaazapentacyclo[11.11.11.$0^{4.9}0^{15,20}0^{25.30}$]ditriaconta-3,9,14,20,24,30-hexaene(2−)iron(II) (7e). Complex $[Fe(H_2Nx)_3]Cl_2$ (0.3 g, 0.54 mmol) was dissolved/suspended in acetonitrile (1 mL), and a solution of Et_3N (0.11 g, 1.1 mmol) and boronate **6e** (0.25 g, 1.1 mmol) in acetonitrile (2 mL) was added dropwise with stirring under argon. The reaction mixture was stirred for 3 h and left for 16 h at 4 °C. The target complex was isolated as described above for clathrochelate **7a**. The yield was 0.15 g (41%). Found (%): C, 55.96; H, 6.85; N, 12.15; Fe, 8.00. $C_{32}H_{46}N_6O_6B_2Fe$. Calculated (%): C, 55.84; H, 6.75; N, 12.21; Fe, 8.11. Mass spectrum: *m/z* 688 $[M]^{\bullet+}$. ^1H NMR ($CDCl_3$), δ: 1.16 (d, 6 H, MeCH (R_B), $J_{H,H}$ = 6.9 Hz); 1.72 (s, 6 H, Me (R_B)); 1.79 (br.s, 12 H, β-CH_2 (Nx)); 2.88 (br.s, 12 H, α-CH_2 (Nx)); 3.67 (m, 2 H, >CH (R_B)); 5.02 (m, 4 H, =CH_2 (R_B)); 5.29 (s, 2 H, BCH (R_B)); 5.96 (m, 2 H, =CH (R_B)). $^{13}C\{^1H\}$ NMR ($CDCl_3$), δ: 17.4 (C(3)H_3 (R_B)); 20.4 (C(2)H_3 (R_B)); 21.6 (β-CH_2 (Nx)); 26.1 (α-CH_2 (Nx)); 41.7 (>CH); 112.3 (=CH_2 (R_B)); 143.7 (=CH (R_B)); 150.9 (C=N); 153.1 (=CMe (R_B)). IR (KBr), ν/cm^{-1}: 930, 1045, 1059 (N—O), 1117 m (B—O), 1574 (C=N), 1630, 1641 (C=C). UV-Vis ($CHCl_3$), λ_{max}/nm (ε · 10^{-3}/L mol^{-1} cm^{-1}): 249 (9.7), 284 (10), 297 (2.7), 430 (4.5), 449 (14).

X-ray diffraction study. Dark orange crystals of complexes **7c** and **7d** suitable for X-ray diffraction experiment were prepared by slow evaporation at room temperature of saturated solutions of these clathrochelates in a methylene chloride—hexane (1 : 1) mixture.

The following systems were chosen for isothermic crystallization of clathrochelate **7a** at room temperature: methylene chloride—hexane (resulting crystals contain no solvent molecules), chloroform—heptane (solvate **7a** · $CHCl_3$), and benzene—isooctane (solvate **7a** · C_6H_6).

The low-temperature X-ray diffraction experiment was carried out with Bruker SMART 1K CCD (**7a**, **7a** · C_6H_6, **7c,d**) and

* R_B is the $CH_2=C(R^1)C(R^2)C(R^3)=CH_2$ substituent at the boron atom.

Bruker APEX II CCD (**7a**·$CHCl_3$) automated diffractometers equipped with a graphite monochromator (Mo-Kα radiation, λ = 0.71073 Å). The SAINT Plus and SADABS programs[23,24] were used for processing of the initial set of experimental intensities. The structures were solved by the direct method and refined by the full-matrix least-squares method against F^2 in the anisotropic approximation for non-hydrogen atoms. Positions of hydrogen atoms were located from the difference Fourier synthesis and refined by the riding model with $U_{iso}(H) = nU_{eq}(C)$, where n = 1.5 for methyl groups and 1.2 for other groups and $U_{eq}(C)$ is the equivalent isotropic factor of the pivot carbon atom. All calculations were performed using the SHELXTL PLUS5 program package.[25] The coordinates of atoms are deposited with the Cambridge Structural Database. The crystallographic data and refinement parameters for crystals **7a**, **7a**·$CHCl_3$, **7a**·C_6H_6, and **7c,d** are presented in Table 4.

To obtain the experimental function of the electron density distribution in the analytical form, the multipole refinement of X-ray diffraction data was performed in terms of the Hansen—Coppens model[26] using the XD program package.[27] In the multipole refinement, the coordinates, anisotropic thermal parameters, and multipole parameters to the octapole level (l = 3) were refined for all non-hydrogen atoms, and the for the iron atom the latter were refined to the hexadecapole level (l = 4). Positions of hydrogen atoms and their isotropic thermal parameters were not refined. The refinement was performed by the full-matrix least-squares method against F_{hkl}. Before the refinement, all C—H distances were normed to ideal values of 1.08 Å. In the multipole refinement of hydrogen atoms, the expansion to the dipoles (l = 2) was used taking into account cylindrical symmetry. Validity of the obtained anisotropic parameters of atomic displacements was estimated by the Hirshfeld test,[28] according to which all the C—C, N—O, B—O, and B—C bonds in the clathrochelate, as well as the C—Cl bonds in the main component of the disordered chloroform molecule, are rigid: the differences between the root-mean-square displacements (Δ) do not exceed $11 \cdot 10^{-4}$ Å^2. Note that the corresponding Δ values for the Fe—N bonds in the coordination compounds were systematically higher ($17 \cdot 10^{-4}$—$19 \cdot 10^{-4}$ Å^2).[29] The results of the multipole refinement were R = 0.0313, wR = 0.0259, GOOF = 0.780 for 30540 reflections with $I > 3\sigma(I)$ and $\sin\theta/\lambda > 1.08$ Å^{-1}. The residual electron density value did not exceed 0.20 e Å^{-3} and

Table 4. Selected crystallographic data and refinement parameters for compounds **7a**, **7a**·$CHCl_3$, **7a**·C_6H_6, and **7c,d**

Parameter	**7a**	**7a**·$CHCl_3$	**7a**·C_6H_6	**7c**	**7d**
Empirical formula	$C_{40}H_{46}B_2FeN_6O_6$	$C_{40}H_{46}B_2FeN_6O_6 \cdot CHCl_3$	$C_{40}H_{46}B_2FeN_6O_6 \cdot 1.5C_6H_6$	$C_{30}H_{42}N_6O_6B_2Fe$	$C_{32}H_{46}N_6O_6B_2Fe$
Molecular weight	784.30	903.67	901.46	660.17	688.22
Space group	$P\bar{1}$	$P\bar{1}$	$P\bar{1}$	$C2/c$	$P\bar{1}$
T/K	120	273	120	120	120
a/Å	9.8575(7)	11.9820(6)	9.0872(7)	23.500(2)	9.2494(11)
b/Å	13.1130(9)	13.5270(6)	15.073(1)	13.1937(13)	12.6572(14)
c/Å	14.537(1)	13.7398(6)	17.471(1)	10.2731(10)	15.4314 (7)
β/deg	83.019(2)	96.253(1)	94.001(2)	90.108(2)	98.488(3)
V/Å^3	1865.3(2)	2132.9(2)	2247.0(3)	3158.3(5)	1668.0(3)
Z	2	2	2	4	2
d_{calc}/g cm^{-3}	1.396	1.407	1.332	1.377	1.370
Color, habit	Dark orange, plate	Dark orange, plate	Dark orange, prism	Red, plate	Red, plate
Dimensions/mm^3	0.20×0.35×0.50	0.30×0.20×0.15	0.25×0.40×0.50	0.40×0.30×0.25	0.40×0.30×0.25
μ/cm^{-1}	4.62	5.95	3.93	5.26	5.05
$2\theta_{max}$/deg	58	110	58	57	47
Total number of reflections	20681	119084	25158	15943	14473
Number of independent reflections (R_{int})	9778 (0.0447)	52943 (0.0364)	11894 (0.0344)	3791 (0.0228)	6398 (0.0733)
R_1 (against F for reflections with $I > 2\sigma(I)$)	0.0457 (6336)	0.0430 (35777)	0.0445 (9012)	0.0401 (3411)	0.1019 (4216)
wR_2 (against F^2 for all reflections)	0.1008	0.1228	0.1007	0.0856	0.1180
Number of refined parameters	515	569	596	213	424
Weighed scheme	$w^{-1} = \sigma^2(F_o^2) + (aP)^2 + bP$, где $P = 1/3(F_o^2 + 2F_c^2)$				
a	0.0092	0.0564	0.0095	0.0138	0.0030
b	1.5300	0.0115	2.2179	9.6030	0.0205
GOOF	1.013	1.007	1.033	1.014	1.033
F(000)	824	940	950	1392	728
Residual electron density (max/min)/e·Å^{-3}	0.588/−0.472	1.008/−1.048	0.831/−0.420	1.031/−0.604	0.686/−0.596

was observed in the region of a disordered chloroform molecule, whereas in the vicinity of the iron atom the residual electron density did not exceed 0.13 e Å^{-3}.

The approximation in terms of the Thomas—Fermi theory[30] was used to calculate the potential energy density $\nu(\mathbf{r})$ from the X-ray diffraction data. According to this approach, the kinetic energy density ($g(\mathbf{r})$) can be obtained from the expression

$$g(\mathbf{r}) = 3/10(3\pi^2)^{2/3}[\rho(\mathbf{r})]^{5/3} + \\ + (1/72)|\nabla\rho(\mathbf{r})|^2/\rho(\mathbf{r}) + (1/6)\nabla^2\rho(\mathbf{r}),$$

in combination with the local virial theorem[31]

$$2g(\mathbf{r}) + \nu(\mathbf{r}) = (1/4)\nabla^2\rho(\mathbf{r}),$$

which makes it possible to calculate both the potential energy density $\nu(\mathbf{r})$ and local energy density $h_e(\mathbf{r})$. Search for critical points, determination of atomic basins, integration of atomic charges, and calculation in CPs (3, −1) of the topological characteristics $\rho(\mathbf{r})$, including $g(\mathbf{r})$, $h_e(\mathbf{r})$), and $\nu(\mathbf{r})$, were performed using the WinXPRO 1.5.20 program.[32]

This work was financially supported by the Russian Foundation for Basic Research (Project Nos 06-03-32626, 05-03-32953, and 05-03-33268), the Division of Chemistry and Materials Science of the Russian Academy of Sciences (Program Nos 7 and 10), and the President of the Russian Federation (Grant NSh-2878.2006.3).

References

1. Y. Z. Voloshin, N. A. Kostromina, and R. Krämer, *Clathrochelates: Synthesis, Structure and Properties*, Elsevier, Amsterdam, 2002.
2. S. C. Jackels and N. J. Rose, *Inorg. Chem.*, 1972, **12**, 1232.
3. A. Yu. Nazarenko and Ya. Z. Voloshin, *Zh. Neorg. Khim.*, 1984, **28**, 1776 [*J. Inorg. Chem. USSR*, 1984, **28** (Engl. Transl.)].
4. Ya. Z. Voloshin, A. Yu. Nazarenko, and V. V. Trachevskii, *Ukr. Khim. Zh.* [*Ukrainian Chemical Journal*], 1985, **51**, 121 (in Russian).
5. H. C. Rai, A. K. Jena, and B. Sahoo, *Inorg. Chim. Acta*, 1979, **35**, 29.
6. M. K. Robbins, D. W. Naser, J. L. Heiland, and J. J. Grzybowski, *Inorg. Chem.*, 1985, **24**, 3381.
7. J. J. Grzybowski, *Inorg. Chem.*, 1985, **24**, 1125.
8. Y. Z. Voloshin, N. A. Kostromina, and A. Y. Nazarenko, *Inorg. Chim. Acta*, 1990, **170**, 181.
9. Y. Z. Voloshin, M. I. Terekhova, Y. G. Noskov, V. E. Zavodnik, and V. K. Belsky, *Anales de Química Int. Ed.*, 1998, **94**, 142.
10. B. M. Mikhailov and Yu. N. Bubnov, *Organoboron Compounds in Organic Synthesis*, Harwood Acad. Publishers, London—New York, 1984.
11. B. M. Mikhailov, Yu. N. Bubnov, S. A. Korobeinikova, and V. S. Bogdanov, *Zh. Obshch. Khim.*, 1970, **40**, 1321 [*J. Gen. Chem. USSR*, 1970, **40** (Engl. Transl.)
12. S. Yu. Erdyakov, A. V. Ignatenko, T. V. Potapova, M. E. Gurskii, and Yu. N. Bubnov, *Tez. I Molodezhnoi konf. IOKh RAN* [*Abstr. I Youth Conf. of the Institute of Organic Chemistry, Russian Academy of Sciences*] (*Moscow, March 31—April 1, 2005*), Moscow, 2005, 41 (in Russian).
13. S. Y. Erdyakov, A. V. Ignatenko, T. V. Potapova, M. E. Gurskii, and Y. N. Bubnov, *Abstr. XII Intern. Conf. on Boron Chemistry "Imeboron XII"* (*Japan, Sendai, September 11—15, 2005*), 2005, SP-B02.
14. S. Le Serre and J.-C. Guillemin, *Organometallics*, 1997, **16**, 5844; Yu. N. Bubnov, N. Yu. Kuznetsov, F. V. Pastukhov, and V. V. Kublitsky, *Eur. J. Org. Chem.*, 2005, 4633.
15. Y. Z. Voloshin, T. E. Kron, V. K. Belsky, V. E. Zavodnik, Y. A. Maletin, and S. G. Kozachkov, *J. Organomet. Chem.*, 1997, **536/537**, 207.
16. S. A. Kubow, K. J. Takeuchi, J. J. Grzybowski, A. J. Jircitano, and V. L. Goedken, *Inorg. Chim. Acta*, 1996, **241**, 21.
17. Y. Z. Voloshin, O. A. Varzatskii, A. I. Stash, V. K. Belsky, Y. N. Bubnov, I. I. Vorontsov, K. A. Potekhin, M. Y. Antipin, and E. V. Polshin, *Polyhedron*, 2001, **20**, 2721.
18. Ya. Z. Voloshin, O. A. Varzatskii, I. I. Vorontsov, M. Yu. Antipin, A. Yu. Lebedev, A. S. Belov, and A. V. Pal´chik, *Izv. Akad. Nauk, Ser. Khim.*, 2003, 1469 [*Russ. Chem. Bull., Int. Ed.*, 2003, **52**, 1552].
19. F. Cortés-Guzmán and R. F. W. Bader, *Coord. Chem. Rev.*, 2005, **249**, 633.
20. P. Macchi and A. Sironi, *Coord. Chem. Rev.*, 2003, **238**, **239**, 383.
21. K. I. Turta, R. A. Stukan, I. I. Bulgak, L. G. Batyr, and L. D. Ozol, *Koord. Khim.*, 1978, **4**, 1391 [*Sov. J. Coord. Chem.*, 1978, **4** (Engl. Transl.)].
22. S. Yu. Erdyakov, S. V. Stefanyuk, A. V. Ignatenko, M. E. Gurskii, and Yu. N. Bubnov, *Tez. II Molodezhnoi konf. IOKh RAN* [*Abstr. II Youth Conf. of the Institute of Organic Chemistry, Russian Academy of Sciences*] (*Moscow, April 13—14, 2006*), Moscow, 2006, 46 (in Russian).
23. *SAINTPlus. Data Reduction and Correction Program, v. 6.01*, Bruker AXS, Madison (Wisconsin, USA), 1997—1998.
24. *SADABS v. 2.01, Bruker/Siemens Area Detector Absorption Correction Program*, Bruker AXS, Madison (Wisconsin, USA), 1999.
25. *SHELXTL v. 5.10, Structure Determination Software Suite*, Bruker AXS, Madison (Wisconsin, USA), 1999.
26. N. K. Hansen and P. Coppens, *Acta Crystallogr.*, 1978, **A34**, 909.
27. T. Koritsanszky, S. T. Howard, T. Richter, P. Macchi, A. Volkov, C. Gatti, P. R. Mallinson, L. J. Farrugia, Z. Su, and N. K. Hansen, *XD — A Computer Program Package for Multipole Refinement and Topological Analysis of Charge Densities from Diffraction Data*, 2003.
28. F. L. Hirshfeld, *Acta Crystallogr.*, 1976, **A32**, 239.
29. K. A. Lyssenko, A. A. Korlyukov, D. G. Golovanov, S. Yu. Ketkov, and M. Yu. Antipin, *J. Phys. Chem. A*, 2006, 6545.
30. D. A. Kirzhnitts, *Zh. Teor. Eksp. Fiz.*, 1957, **5**, 64 [*J. Exp. Theor. Phys.*, 1957, **5** (Engl. Transl.)].
31. R. F. W. Bader, *Atoms in Molecules. A Quantum Theory*, Clarendron Press, Oxford, 1990.
32. A. Stash and V. Tsirelson, *WinXPRO — a Program for Calculation of the Crystal and Molecular Properties Using The Model Electron Density*, Moscow (Russia), 2001.

Received July 31, 2006